Report on the proposal "Investigation of magnetic coupling in the double perovskite La_2CrWO_6"

Ref No. 28343
Final No. HE-3796

Half metallic antiferromagnets (HM-AFM) have been predicted by van Leuken and de Groot [1] as materials with 100% spin polarization of charge carriers and zero net magnetization. Heusler alloys[2], thiospinels[3], and double perovskites[4] have been suggested as HM-AFMs from density functional theory. Double perovskites crystallize in a simple structure and are compatible to the large family of functional perovskites. They are described by the general formula $A_2BB'O_6$ where A is an earth alkaline or rare earth element and B (B') a transition metal. In HM-AFMs, the magnetic moments of B and B' align antiferromagnetically. Perhaps the biggest obstacle through synthesizing double perovskites is the antisite disorder where the B and B' cations occupy the wrong atomic sites in the crystal. The presence of antisite disorder may alter completely the physical properties of double perovskites. By combining 3d (B) with 4d and 5d (B') transition metals, a structure with higher cationic order may form due to the difference in the ionic radii. Pickett *et al.* predicted two double perovskites, namely K_2MnRhO_6 and La_2CrWO_6 (LCWO) with d^3-d^3 configuration[5]. *Ab initio* calculations predict an undistorted tetragonal structure of LCWO with a = 4.00 Å. In this case, spin-orbital coupling does not affect the magnetic compensation, and even a large Coulomb repulsion (7 eV for Cr and 4 eV for W) does not destroy half-metallicity. The predicted total magnetic moment remains below 0.10 μ_B/f.u.. From a thermodynamics point of view, the formation of a W^{3+} state in LCWO is a real challenge. We have used the thin film approach as the synthesis method to circumvent thermodynamic equilibrium. We have synthesized LCWO by pulsed laser deposition with predominant W^{3+} state. However, the antisite disorder in our thin films is considerable. By optimizing the partial pressure of oxygen and deposition temperature, we have synthesized LCWO thin films with 65% cationic ordering. We have characterized the crystal structure, thin film-substrate epitaxial relation and degree of ordering using X-ray diffraction technique. The stoichiometry of the films was evaluated by X-ray photoelectron spectroscopy and Rutherford backscattering spectroscopy.

In order to reveal the effect of antisite disorder on magnetic and electronic structure of LCWO thin films, we performed XANES at Cr K-edge and W $L_{2,3}$-edges at European Synchrotron Radiation Facility (ESRF, beamline ID12). Therefore, we have measured two LCWO thin films deposited on $SrTiO_3$ (STO) substrate with 10 and 65% cationic order which we call them disorder (DO) and relatively ordered (RO) LCWO thin films, respectively.

The spectra were recorded using the total fluorescence yield detection mode. X-ray magnetic circular dichroism (XMCD) signals at the W $L_{2,3}$-edges were obtained as direct difference between consecutive XANES scans registered with opposite helicities of the incoming X-ray beam. To ensure that the XMCD spectra are free from any experimental artifacts, the data were collected for both directions of applied magnetic field of 17T (parallel and antiparallel to the X-ray beam). The monochromatic X-ray beam was to 95% circularly polarized. The measurements were performed at 5 and 300 K. Due to detection of remarkably intense diffraction peaks of STO substrate, the

measurement range was restricted and could not be extended to the range of 10 eV below and above the edges. Thus the spectra were normalized to the edges. Since the samples were measured in backscattering geometry, first the spectra were normalized and then corrected for self-absorption effects. The edge jump intensity ratio L_3/L_2 was then corrected to 2.19/1[6]. This is different from the statistical 2:1 branching ratio due to the difference in the radial matrix elements of the $2p_{1/2}$ to $5d$ (L_2) and $2p_{3/2}$ to $5d$ (L_3) transitions.

In order to determine the valence state of Cr cations, we have measured XANES at Cr *K*-edge since this edge is very sensitive to the oxidation state of the probed element. Normalized spectra of RO- and DO-LCWO thin films are shown in Figure 1 along with the same spectra of thin films of double perovskite Sr_2CrWO_6 (SCWO) and single perovskite $LaCrO_3$ (LCO).

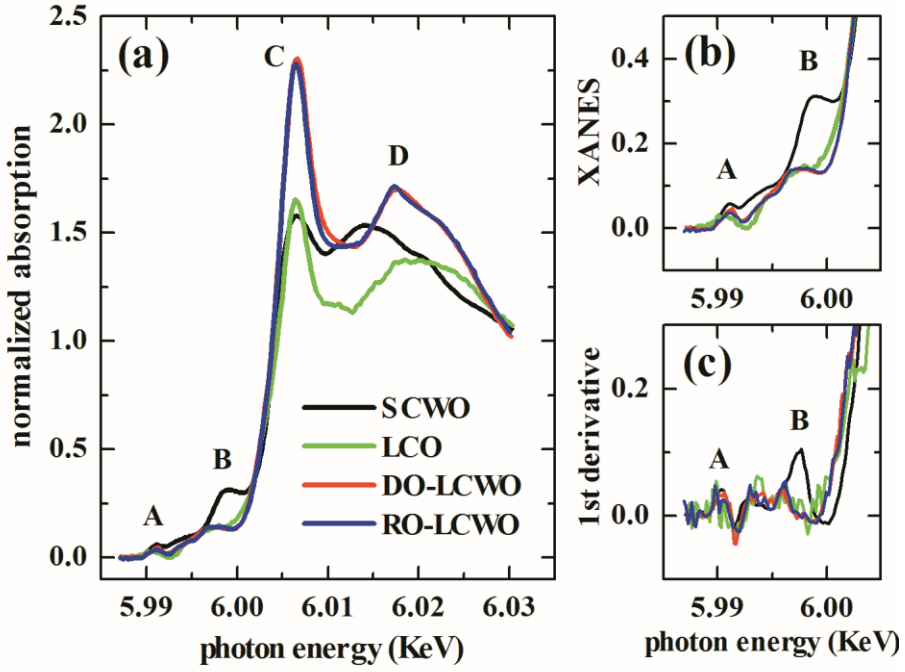

Figure 1 (a) XANES spectra of Cr *K*-edge of DO- and RO-LCWO thin films. Spectra of Sr_2CrWO_6 (SCWO) and $LaCrO_3$ (LCO) thin films are included. (b) Magnification of the pre-edge part of the XANES spectra. (c) First derivatives of the XANES spectra. Pre-edge features are denoted as A and B, edge position is marked with C, and resonances above the edge are denoted with D.

The edge position (marked with C) has been attributed to the transition of $1s \rightarrow 4p$ which is characteristic for the Cr oxidation state. For all spectra, the edge position occurs at 6003 eV suggesting the same valence state +3 in agreement with literature[7]. Resonances above the edge marked with D are quite dissimilar for the different spectra. The pre-edge features assigned with A and B are attributed to quadrupole allowed transitions of $1s \rightarrow 3d$. The feature A (Figure 1b) at 5991 eV, is similar in all cases and corresponds to a pure quadrupole transition[8], thus, the compounds with identical oxidation state of Cr exhibit almost identical feature. In contrast, the feature B is most intense for the SCWO thin film. The first derivatives of the XANES spectra shown in Figure 1c give a clear image of the differences in feature B. This feature is similar for LCO and LCWO spectra, both, in terms of energy and intensity. Since a single and a double perovskite show a

similar feature, we rule out ascribing this feature to the presence or lack of *B*-site order. Furthermore, it has been reported that doping a trivalent cation on the A-site of Cr-Re based DPs decreases the intensity of feature B and shifts its energy to lower values[7]. Hence, this feature can be related to the hybridization of Cr3*d* - O2*p* electrons which itself depends on the radius of the *A*-site cation.

XANES spectra at W$L_{2,3}$-edges were measured for both RO- and DO- LCWO samples (Figure 2). For comparison, the spectra of SCWO are presented.

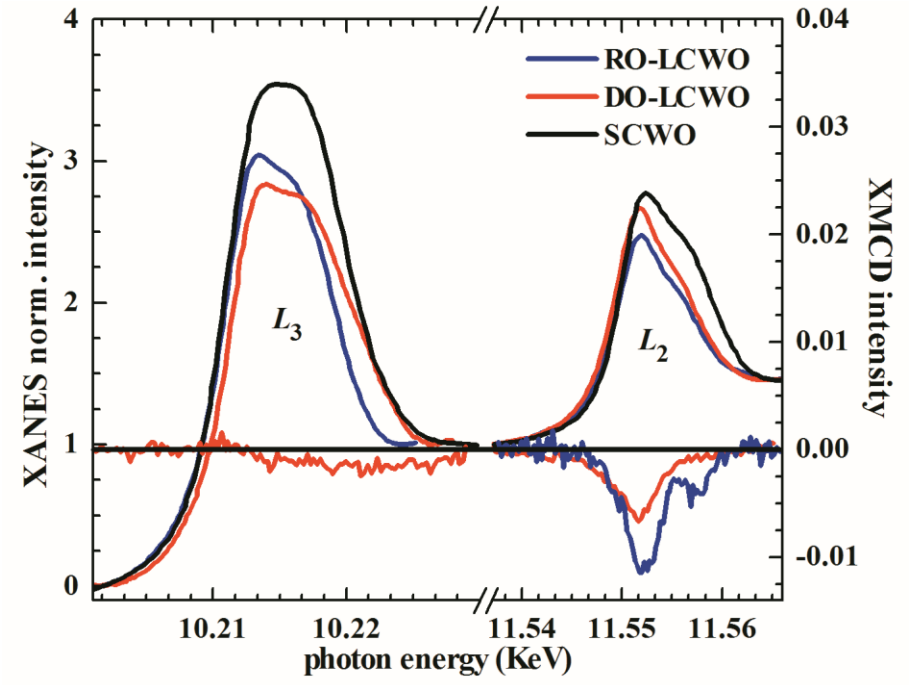

Figure 2 Normalized XANES (left-hand axis) and XMCD (right-hand axis) spectra at W $L_{2,3}$-edges of RO- and DO LCWO thin films recorded at 5K under an applied magnetic field of 17 T. Spectra of the SCWO thin film are included for comparison. Normalized L_2 edge spectra are plotted after applying a L_3/L_2 ratio coefficient of 2.19.

Double peaks at the L_2 and L_3 edges are attributed to crystal field splitting. L_2 and L_3 edges probe the transitions $2p_{1/2} \rightarrow 5d_{3/2}$ and $2p_{3/2} \rightarrow 5d_{3/2}$, $5d_{5/2}$, respectively. These edges are less structured comparing to the *K*-edge. However, it is very common to ascribe the area of the spectrum to the number of holes in the *d* shell, and consequently, the valence state of the element. By comparing the sum of the calculated areas of L_2 and L_3 spectra (see Table I), we notice that the spectra of the LCWO thin films exhibit a smaller area than the SCWO film. The oxidation state of W in A_2CrWO_6 DPs (A = Ca, Sr) is +5[9], thus, the valence state of W in LCWO thin films should be less than +5. The sample with the higher degree of cationic order shows a slightly larger number of *d*-holes.

In total, we have shown unambiguously that the oxidation state of Cr is +3. Considering the stable oxidation state of La^{3+}, we conclude that we have, as predicted, a rare W^{3+} state in the deposited thin films. The percentage of W^{3+} is slightly reduced from 100% due to the presence of cationic vacancies which can be compensated by an increase in W valence state.

Table I Calculated areas (**A**) of the XANES spectra at W L_2 and L_3 edges. Spin, orbital, and total magnetic moment of W are listed (m_s, m_l, and m_{tot}). The values are compared to Sr_2CrWO_6 bulk results.

	$\mathbf{A}_{L_2}$ (eV)	$\mathbf{A}_{L_3}$(eV)	$\mathbf{A}_{L_2+L_3}$(eV)	m_s (μ_B/W)	m_l (μ_B/W)	$\lvert m_l / m_s \rvert$	m_{tot} (μ_B/W)
LCWO-RO	22.34	22.73	45.07	-0.05 ± 0.01	0.02 ± 0.01	0.33	-0.03 ± 0.01
LCWO-DO	26.02	23.08	49.10	-0.03 ± 0.01	0.01 ± 0.01	0.33	-0.02 ± 0.01
SCWO	30.26	30.77	61.03	-0.33 ± 0.02	-0.12 ± 0.02	0.35	-0.21 ± 0.01

The XMCD signals at the L_2 and L_3 edges of W are shown in Figure 2. For 5*d* transition metals, the XMCD intensity at the L_3 edge is about 10 times weaker than at the L_2 edge. Noticing the intensity of the XMCD signal at the L_2 edge, the resulting XMCD signal at the L_3 edge is almost zero. The XMCD signal from the L_2 edge unambiguously shows a negative sign of the W magnetic moment. The only possible explanation for this negative sign is an antiferromagnetic coupling between Cr and W neighboring pairs according to the kinetic energy driven exchange model[10, 11]. Another important result is that the thin film with higher degree of order shows also a larger average total magnetic moment on the W sites. This is expected since a higher degree of order increases the magnetic coupling between Cr and W. We have measured XMCD at 5 and 300 K, as well as in magnetic fields of 5 and 17 T. We have not observed any significant change in the amplitude of the XMCD signal. This signifies that the induced magnetic moment of W is independent within the range of applied temperatures and saturates in a magnetic field of 5 T. This means that the origin of the XMCD signal does not arise from the field induced paramagnetic effect but originates from a ferromagnetic state. Using the sum rules, spin, orbital, and total magnetic moments of the 5*d* shell of W were calculated (Table I). In the analysis, we have neglected the contribution of the dipole magnetic term. In accordance with Hund's third rule, spin and orbital moments of W are antiparallel.

The predicted value of the W3+ total magnetic moment for a perfectly ordered sample is 1.5 μ_B /W atom. For the sample with higher degree of order, we only observe a total magnetic moment of m_{tot}=-0.03 μ_B /W atom which is 50 times smaller than the ideal value. Note that even in highly ordered bulk Sr_2CrWO_6 material consisting of W^{5+} cations, only m_{tot} =-0.21 μ_B /W atom has been observed[12]. Our result indicates that the reduction of the magnetic moment due to cationic disorder does not depend linearly on the antisite disorder, but is reduced much stronger. This is most likely due to the formation of antiferromagnetic clusters resulting from overlapping antisite disordered regions with Cr-Cr and W-W interactions. However, the observation of the *opposite* total magnetic moment of W with respect to the external magnetic field shows that the antiferromagnetic coupling between Cr and W is dominant in parts of the structure. Since it is also obvious that a higher degree of cationic order leads to an increase in total W magnetic moment, we conclude that a highly ordered sample should come much closer to the predicted antiferromagnetic state. The observation of a relatively large orbital magnetic moment (the ratio of orbital to spin magnetic moment is similar for all samples ~ 0.3 - 0.4) implies that a fully antiferromagnetic state cannot be obtained in Re and W based double perovskites[9].

1. H. van Leuken and R. A. de Groot, Phys Rev Lett **74** (7), 1171-1173 (1995).
2. I. Galanakis, K. Özdoğan, E. Şaşıoğlu and B. Aktaş, Phys Rev B **75** (17), 172405 (2007).
3. M. Nakao, Phys Rev B **74** (17), 172404 (2006).

4. W. E. Pickett, Phys Rev B **57** (17), 10613-10619 (1998).
5. V. Pardo and W. E. Pickett, Phys Rev B **80** (5), 054415 (2009).
6. F. Wilhelm, P. Poulopoulos, H. Wende, A. Scherz, K. Baberschke, M. Angelakeris, N. K. Flevaris and A. Rogalev, Phys Rev Lett **87** (20), 207202 (2001).
7. J. Blasco, J. M. Michalik, J. García, G. Subías and J. M. De Teresa, Phys Rev B **76** (14), 144402 (2007).
8. H. Wu, Phys Rev B **64** (12), 125126 (2001).
9. P. Majewski, S. Geprägs, A. Boger, M. Opel, A. Erb, R. Gross, G. Vaitheeswaran, V. Kanchana, A. Delin, F. Wilhelm, A. Rogalev and L. Alff, Phys Rev B **72** (13), 132402 (2005).
10. J. B. Philipp, P. Majewski, L. Alff, A. Erb, R. Gross, T. Graf, M. S. Brandt, J. Simon, T. Walther, W. Mader, D. Topwal and D. D. Sarma, Phys Rev B **68** (14), 144431 (2003).
11. D. D. Sarma, P. Mahadevan, T. Saha-Dasgupta, S. Ray and A. Kumar, Phys Rev Lett **85** (12), 2549-2552 (2000).
12. Z. Fang, K. Terakura and J. Kanamori, Phys Rev B **63** (18), 180407 (2001).